Abnormal metabolic network activity in REM sleep behavior disorder

Florian Holtbernd, MD*
Jean-François Gagnon, PhD*
Ron B. Postuma, MD
Yilong Ma, PhD
Chris C. Tang, MD, PhD
Andrew Feigin, MD
Vijay Dhawan, PhD
Mélanie Vendette, MSc
Jean-Paul Soucy, MD
David Eidelberg, MD‡
Jacques Montplaisir, MD, PhD‡

Correspondence to Dr. Eidelberg: david1@nshs.edu

ABSTRACT

Objective: To determine whether the Parkinson disease–related covariance pattern (PDRP) expression is abnormally increased in idiopathic REM sleep behavior disorder (RBD) and whether increased baseline activity is associated with greater individual risk of subsequent phenoconversion.

Methods: For this cohort study, we recruited 2 groups of RBD and control subjects. Cohort 1 comprised 10 subjects with RBD (63.5 ± 9.4 years old) and 10 healthy volunteers (62.7 ± 8.6 years old) who underwent resting-state metabolic brain imaging with ^{18}F-fluorodeoxyglucose PET. Cohort 2 comprised 17 subjects with RBD (68.9 ± 4.8 years old) and 17 healthy volunteers (66.6 ± 6.0 years old) who underwent resting brain perfusion imaging with ethylcysteinate dimer SPECT. The latter group was followed clinically for 4.6 ± 2.5 years by investigators blinded to the imaging results. PDRP expression was measured in both RBD groups and compared with corresponding control values.

Results: PDRP expression was elevated in both groups of subjects with RBD (cohort 1: $p < 0.04$; cohort 2: $p < 0.005$). Of the 17 subjects with long-term follow-up, 8 were diagnosed with Parkinson disease or dementia with Lewy bodies; the others did not phenoconvert. For individual subjects with RBD, final phenoconversion status was predicted using a logistical regression model based on PDRP expression and subject age at the time of imaging ($r^2 = 0.64$, $p < 0.0001$).

Conclusions: Latent network abnormalities in subjects with idiopathic RBD are associated with a greater likelihood of subsequent phenoconversion to a progressive neurodegenerative syndrome.

Neurology® 2014;82:620–627

GLOSSARY

DLB = dementia with Lewy bodies; **ECD** = ethylcysteinate dimer; **FDG** = ^{18}F-fluorodeoxyglucose; **MSA** = multiple system atrophy; **PD** = Parkinson disease; **PDRP** = Parkinson disease–related covariance pattern; **RBD** = REM sleep behavior disorder; **VOI** = volume of interest.

REM sleep behavior disorder (RBD) can occur in isolation, but many individuals develop a defined neurodegenerative syndrome within 5 years of diagnosis.[1,2] Most often, phenoconversion is a manifestation of underlying Lewy body pathology as seen in idiopathic Parkinson disease (PD), dementia with Lewy bodies (DLB), and multiple system atrophy (MSA).[3]

Many neurodegenerative diseases, including those associated with RBD, exhibit stereotyped changes in brain structure and function that occur at the systems level.[4] Indeed, network analysis of resting-state functional imaging data has revealed distinct spatial covariance topographies that characterize these disorders.[5–7] Idiopathic PD is a case in point. This disorder is associated with a highly reproducible disease-related metabolic brain network, known as the PD-related covariance pattern (PDRP).[5,7–9] The PDRP topography (figure 1) is characterized by increases in pallidothalamic, pontine, and cerebellar metabolic activity and by reductions in premotor and parietal association regions. Progressive motor disability in patients with PD is accompanied by continuous increases in PDRP expression,[5,10] consistent with a close relationship between

Supplemental data at www.neurology.org

*These authors contributed equally to this work.

‡These authors share senior authorship.

From the Center for Neurosciences (F.H., Y.M., C.C.T., A.F., V.D., D.E.), The Feinstein Institute for Medical Research, Manhasset, NY; Center for Advanced Research in Sleep Medicine (J.-F.G., R.B.P., M.V., J.M.), Hôpital du Sacré-Coeur de Montréal; Department of Psychology (J.-F.G., M.V.), Université du Québec à Montréal; Department of Neurology (R.B.P.), Montreal General Hospital; Montreal Neurological Institute (J.-P.S.), McGill University; and Department of Psychiatry (J.M.), University of Montreal, Montréal, Canada.

Go to Neurology.org for full disclosures. Funding information and disclosures deemed relevant by the authors, if any, are provided at the end of the article.

Figure 1 Parkinson disease–related spatial covariance pattern

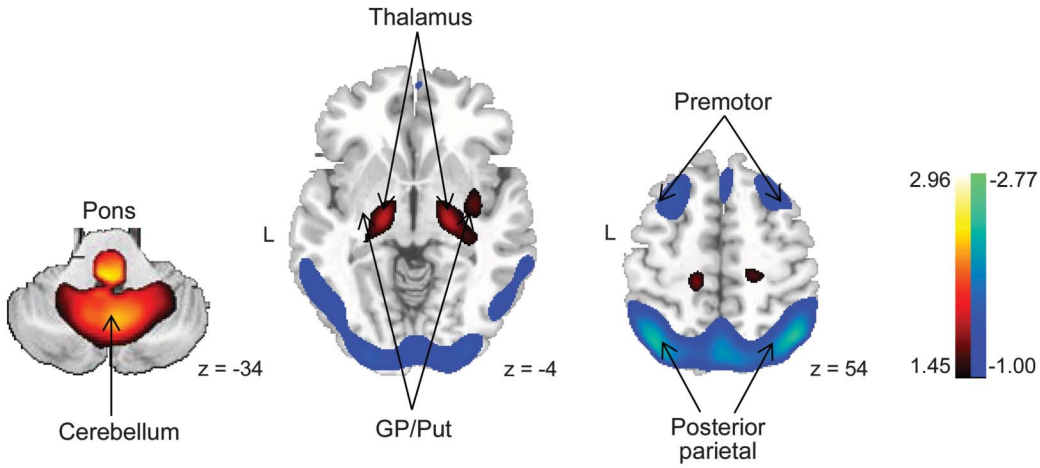

This abnormal brain network is characterized by increased metabolic activity in the pons, cerebellum, globus pallidus internus (GP), putamen (Put), ventral thalamus, and primary motor cortex and relative reductions in the lateral premotor and parietal association regions. The color stripe represents region weights (voxel loadings) on the network. Positive voxel weights (denoting regions with increased metabolic activity) are color-coded from red to yellow. Negative voxel weights (denoting regions with reduced metabolic activity) are color-coded from blue to green. The left side (L) is indicated for each slice. Coordinates correspond to the Montreal Neurological Institute standard space.

network activity and clinical manifestations in individuals with this disorder.[5,6] Nonetheless, network activity was found to be elevated in the "presymptomatic" hemisphere (i.e., ipsilateral to the symptomatic body side) in patients with early-stage PD with unilateral motor involvement ("hemi-PD"), anteceding the onset of contralateral limb manifestations by several years.[11]

In this study, we used functional imaging to determine whether analogous prodromal network abnormalities were present in individuals with idiopathic RBD and whether abnormal network expression was a predictor of subsequent phenoconversion.

METHODS **Subjects.** We studied 2 discrete groups of subjects with RBD who were diagnosed according to established criteria.[12] Exclusion criteria were signs or symptoms of other neurologic diseases and RBD secondary to other diseases or medication. Cohort 1 comprised 10 subjects with RBD recruited at the sleep disorders clinics of the North Shore-Long Island Jewish Health System (Manhasset, NY) and the Hospital of the University of Pennsylvania (Philadelphia) between November 2010 and May 2013. These individuals and 10 healthy age-matched volunteer subjects (62.7 ± 8.6 years old) underwent metabolic brain imaging with ^{18}F-fluorodeoxyglucose (FDG)-PET to evaluate resting metabolic activity at both the network and region (nodal) levels. Cohort 2 comprised a second group of subjects with RBD who were recruited at the Sleep Disorders Clinic of the Hôpital du Sacré-Coeur de Montréal (Canada) between February 2003 and July 2008. These subjects and 17 healthy age-matched volunteers (66.6 ± 6.0 years old) underwent cerebral perfusion imaging with 99mTc ethylcysteinate dimer (ECD) and SPECT. Limited clinical and imaging data from these subjects have been presented previously.[13,14] In this study, we used the scan data from cohort 2 to validate the functional brain changes discerned in the first cohort.

Scan data from cohort 2 were additionally used to determine whether the presence of baseline functional abnormalities in individuals with idiopathic RBD was associated with subsequent phenoconversion, as determined by the later development of a defined neurodegenerative syndrome. After baseline imaging, subjects with RBD in this cohort were followed annually by a movement disorders neurologist (R.B.P.) and a neuropsychologist (J.-F.G.). Eight members of this cohort subsequently developed parkinsonism, and were diagnosed with either PD (n = 5) or DLB (n = 3) according to established criteria.[15,16] The remaining 9 subjects with RBD in this group did not phenoconvert during the follow-up period.

Apart from the 17 subjects with RBD in cohort 2, we analyzed baseline ECD SPECT data from 3 additional subjects with idiopathic RBD who subsequently developed signs of atypical parkinsonism. These subjects were diagnosed with probable (n = 1) or possible (n = 2) MSA according to consensus criteria.[17] Given that the histopathology of MSA is different from PD/DLB, and that this neurodegenerative phenotype develops less frequently in idiopathic RBD,[12] these subjects were analyzed as a discrete diagnostic category (see below).

Imaging procedures. Cohort 1 subjects underwent metabolic imaging with FDG-PET in an eyes-open resting state as detailed elsewhere.[8] Subjects recruited at North Shore-Long Island Jewish Health System (n = 5) were scanned on a GE Advance tomograph (General Electric, Milwaukee, WI). Subjects recruited at the University of Pennsylvania (n = 5) were scanned on a Biograph 40 mCT-S PET/CT device (Siemens Medical Solutions, Knoxville, TN). Cohort 2 subjects underwent perfusion imaging with ECD SPECT in a similar awake state as previously described.[13] These subjects were scanned using the 3-headed SPECT camera (PRISM system; Picker Co., Cleveland, OH) at Hôpital du Sacré-Coeur de Montréal in Montreal, Canada.

Table 1 Comparisons of metabolic activity in PDRP regions[a]

	Cohort 1 (metabolism)			Cohort 2 (perfusion)				
	RBD (n = 10)	NL (n = 10)	*p* Value	RBD (n = 17)	NL (n = 17)	*p* Value	CON(+)[b] (n = 8)	CON(−)[c] (n = 9)	*p* Value
Positive regions[d]									
Pons: [0, −38, −38]	1.25 ± 0 07	1.16 ± 0.08	0.021[e]	1.39 ± 0.08	1.28 ± 0.09	0.002[e]	1.44 ± 0.07	1.33 ± 0.04	0.001[e]
GP/Put: R [36, −8, −4], L [−36, −8, −4]	1.83 ± 0.07	1.75 ± 0.07	0.016[e]	1.72 ± 0.05	1.68 ± 0.08	0.047[e]	1.73 ± 0.05	1.71 ± 0.06	0.594
Thalamus: R [24, −18, 8], L [−20, −18, 8]	1.48 ± 0.08	1.39 ± 0.09	0.041[e]	1.65 ± 0.05	1.61 ± 0.08	0.061	1.66 ± 0.06	1.64 ± 0.04	0.378
Motor cortex: R [24, −26, 48], L [−14, −28, 54]	1.28 ± 0.08	1.26 ± 0.09	0.578	1.44 ± 0.07	1.41 ± 0.05	0.244	1.44 ± 0.08	1.44 ± 0.07	0.971
Cerebellum: [4, −60, −30]	1.67 ± 0.14	1.56 ± 0.10	0.058	1.89 ± 0.08	1.80 ± 0.13	0.022[e]	1.93 ± 0.08	1.85 ± 0.07	0.061
Negative regions[d]									
Premotor cortex: R [30, 24, 48], L [−26, 24, 50]	1.89 ± 0.09	1.86 ± 0.12	0.574	1.47 ± 0.06	1.48 ± 0.06	0.866	1.48 ± 0.05	1.47 ± 0.07	0.804
Parietal cortex: R [40, −68, 46], L [−40, −64, 46]	1.92 ± 0.09	1.87 ± 0.10	0.242	1.47 ± 0.08	1.47 ± 0.07	0.917	1.44 ± 0.08	1.49 ± 0.07	0.243

Abbreviations: GP = globus pallidus; NL = normal controls; PDRP = Parkinson disease–related covariance pattern; Put = putamen; RBD = REM sleep behavior disorder.
In each region, local activity was globally normalized and presented as the mean ± SD for each nodal volume of interest; see text.
[a] Nodes correspond to areas with high (positive) or low (negative) regional loadings (voxel weights) on the PDRP network.
[b] CON(+) = subjects with RBD who developed clinical signs of either Parkinson disease or dementia with Lewy bodies during the follow-up period.
[c] CON(−) = subjects with RBD who did not phenoconvert during follow-up.
[d] Coordinates of local maxima in Montreal Neurological Institute standard space.
[e] Significant group differences ($p < 0.05$, Student t test).

Network measurements. Preprocessing of the scan data was performed using SPM 5 (Wellcome Department of Cognitive Neurology, London, UK) implemented in MATLAB (MathWorks, Sherborn, MA). Images were spatially normalized and smoothed (full width at half maximum 10 × 10 × 10 mm for FDG-PET; 14 × 14 × 14 mm for ECD SPECT). PDRP expression values, reflecting whole-brain network activity in each subject, were computed using an automated voxel-based algorithm (software available at http://www.fil.ion.ucl.ac.uk/spm/ext/#SSM).[5,9,18] Measurements of whole-brain PDRP expression were standardized by *z* scoring with respect to corresponding values from healthy subjects scanned under the same tomographic conditions. This permitted the comparison of network changes across imaging modalities.[9,18]

In cohort 1, the PDRP scores were standardized based on values computed in FDG-PET scans from the corresponding healthy reference group as described elsewhere.[9,18] We also computed network activity in cohort 1 subjects on a hemisphere-by-hemisphere basis.[11] For each subject, right and left hemisphere PDRP values were *z* scored with respect to corresponding hemispheric measurements from the healthy control group. For RBD and healthy control subjects, right and left hemisphere PDRP measurements were averaged and compared with analogous values computed in the preclinical (ipsilateral) hemispheres of subjects with early-stage PD and unilateral symptoms. This previously reported cohort comprised 15 subjects with hemi-PD who were scanned with FDG-PET at baseline and again, 2 and 4 years later.[11]

In cohort 2, we used the same procedure to compute whole-brain PDRP values in the ECD SPECT data.[19,20] PDRP values computed in this sample were standardized with respect to corresponding measurements from the healthy control subjects for this cohort. As in cohort 1, these automated computations were performed on an individual case basis, blinded to group membership and final clinical status.

In both cohorts, a regional analysis was conducted to assess group differences in resting brain function at the major nodes of the PDRP network. Volumes of interest (VOIs)[8] were defined by 4-mm spheres centered at nodal maxima (table 1) situated in the pons, cerebellum, putamen/globus pallidus, and thalamus and in sensorimotor, lateral premotor, and parietal association cortex. A single midline VOI was placed in the pons and cerebellar vermis; separate right and left VOIs were delineated for the other regions, which were averaged for further analysis. In each VOI, local activity was ratio normalized by the global value for the corresponding scan. Group differences in PDRP expression and in local activity at each node were assessed using 2-tailed Student *t* tests.

Logistical regression analysis. Logistical regression analysis was used to determine whether baseline measurements of PDRP expression correlated with the likelihood of subsequent phenoconversion in the RBD follow-up cohort (cohort 2). In these subjects, the individual network values were sealed before the final clinical status of the participants was released. We first tested a 2-category predictive model in which phenoconverters to PD/DLB (n = 8) were defined as one classification group, while the nonphenoconverters (n = 9) were defined as the other group. We also tested a 3-category model that included the 3 phenoconverters to possible or probable MSA as a separate classification group. Model selection was based on relative goodness of fit as determined by the Akaike Information Criterion.[21] Categorization accuracy was assessed using likelihood-ratio tests. Group differences in PDRP expression and in regional activity at the major network nodes were evaluated using SPSS software (SPSS Inc., Chicago, IL).

Logistical regression analysis was performed using SAS 9.1 software (SAS Institute Inc., Cary, NC). Results were considered significant for $p < 0.05$.

Standard protocol approvals, registrations, and patient consents. Ethical permission for the procedures was obtained from the Institutional Review Board of North Shore University Hospital, Hospital of the University of Pennsylvania, and Hôpital du Sacré-Coeur de Montréal. Written consent was obtained from each participant after a detailed explanation of the procedures.

RESULTS

Clinical follow-up. Demographic and clinical data from cohort 1 and cohort 2 subjects with RBD are summarized in table e-1 on the *Neurology*® Web site at www.neurology.org. For the 8 subjects with RBD in cohort 2 who subsequently were diagnosed with PD/DLB, the mean interval between imaging and time of diagnosis was 3.4 ± 2.1 years (range, 0.4–6.2 years). The mean interval between imaging and final clinical assessment in the nonphenoconverters was 5.6 ± 2.4 years (range, 3.9–11.3 years) and 4.6 ± 2.5 years (range, 0.4–11.3 years) for the whole cohort. Three additional subjects with RBD (50, 61, and 66 years old; Unified Parkinson's Disease Rating Scale motor ratings 0, 2.5, and 2) were diagnosed with possible or probable MSA and developed signs of atypical parkinsonism 4.3, 2.5, and 2.7 years after imaging. (In cohort 1, the mean duration of clinical follow-up after imaging was 1.3 ± 0.7 years [range, 0–2.2 years]; none of the subjects with RBD in this cohort have phenoconverted as of August 2013.)

Elevated PDRP expression in idiopathic RBD. PDRP expression (figure 2, A and B) was elevated in each of the RBD cohorts relative to corresponding healthy control values (cohort 1: 0.83 ± 0.18 [mean ± SE], $p < 0.04$; cohort 2: 1.04 ± 0.23, $p = 0.004$, Student *t* tests). In cohort 1, the range of network values seen in the subjects with RBD was similar for the 2 imaging sites (North Shore: 0.12–1.55; University of Pennsylvania: 0.09–1.38).

In cohort 2, baseline network activity was higher in the subjects with RBD who subsequently phenoconverted to PD or DLB (n = 8) relative to those who did not phenoconvert (n = 9) during the follow-up period ($p < 0.03$). In both cohorts, the subjects with RBD displayed increases in PDRP expression that were similar to values measured in the preclinical hemispheres of patients with early-stage PD with unilateral motor signs (figure 2A, right). Given the concordance of the PDRP changes observed in RBD cohort 1 and cohort 2, the network abnormality was robust (0.96 ± 0.16, $p < 0.001$) when data from the 2 samples were merged.

Figure 2 Elevated network activity in subjects with RBD

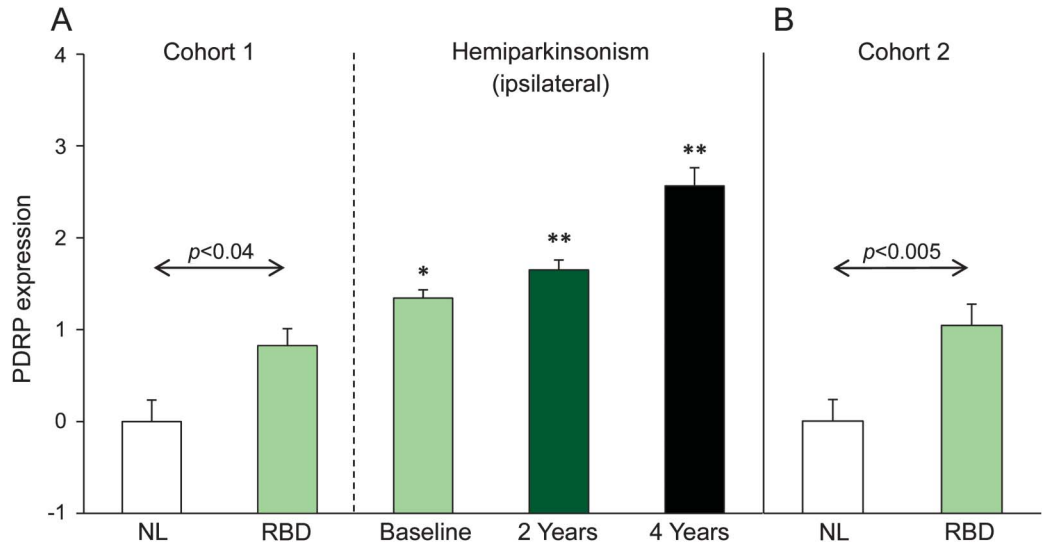

(A) In cohort 1, PDRP expression was quantified in scans of cerebral metabolic activity obtained in 10 subjects with RBD and 10 age-matched NL subjects. In this cohort, PDRP expression (left panel) was abnormally elevated in the RBD group ($p < 0.04$). Network activity in these subjects was comparable to corresponding measures computed in the preclinical hemispheres of a separate cohort of patients with hemiparkinsonism (see text). *$p < 0.005$, **$p < 0.001$ compared with healthy controls; Student *t* test. (B) Similar network changes were observed in cohort 2, in which PDRP expression was quantified in cerebral perfusion scans from 17 individuals with RBD and 17 age-matched NL subjects. Abnormal elevations in network activity were observed in this RBD group ($p = 0.004$) at levels comparable to those measured in the first cohort. In RBD cohort 1 and in the hemi-PD cohort, PDRP scores were computed in FDG-PET scans and standardized with respect to corresponding values from 10 age-matched healthy control subjects. In cohort 2, network expression values computed in ECD SPECT scans were standardized according to the corresponding values from 17 NL subjects (see text). The error bars indicate the SEM. ECD = ethylcysteinate dimer; FDG = ^{18}F-fluorodeoxyglucose; NL = normal control; PD = Parkinson disease; PDRP = Parkinson disease–related covariance pattern; RBD = REM sleep behavior disorder.

Group comparison of resting activity at the major PDRP nodes (table 1) revealed consistent regional changes in both RBD groups. Relative to healthy individuals, subjects with RBD exhibited consistent increases in nodal activity (figure 3, A–D) in the pons (cohort 1: $p = 0.021$; cohort 2: $p = 0.002$) and in the putamen/globus pallidus (cohort 1: $p = 0.016$; cohort 2: $p = 0.047$; Student t tests). Of note, local pontine activity (figure 3B, right) was greater in the subjects with RBD who later phenoconverted to PD/DLB relative to their nonphenoconverter counterparts ($p < 0.001$). Marginal elevations in nodal activity were observed in the thalamus (cohort 1: $p = 0.041$; cohort 2: $p = 0.061$) and the cerebellum (cohort 1: $p = 0.058$; cohort 2: $p = 0.022$). The latter node also exhibited a trend-level increase in the phenoconverters relative to the nonphenoconverters ($p = 0.061$). Differences in functional activity in the RBD and healthy control groups and between phenoconverters and nonphenoconverters were not significant in the other network regions ($p > 0.24$).

Network activity: A predictor of later phenoconversion. Using logistic regression, we first constructed a 2-category predictive model based on PDRP expression in which each subject was classified as either likely to phenoconvert to PD or DLB or as unlikely to phenoconvert. This model exhibited a good fit to the data, accounting for 27.6% of the variance in final clinical status ($p < 0.02$). Review of the individual data revealed high baseline network activity (subject scores ≥0.90) in each of the 8 subjects with RBD who subsequently phenoconverted to PD or DLB. Network elevations of similar magnitude were, however, also seen in 3 of the 9 subjects who did not phenoconvert during the follow-up period (figure 4A, arrows). A second predictive model based on subject age at the time of imaging had comparable goodness of fit, accounting for 23.7% of the variance in outcome ($p < 0.04$). Notably, the correlation between these 2 variables was not significant ($p = 0.58$), suggesting their independence as predictors

Figure 3 Nodal analysis

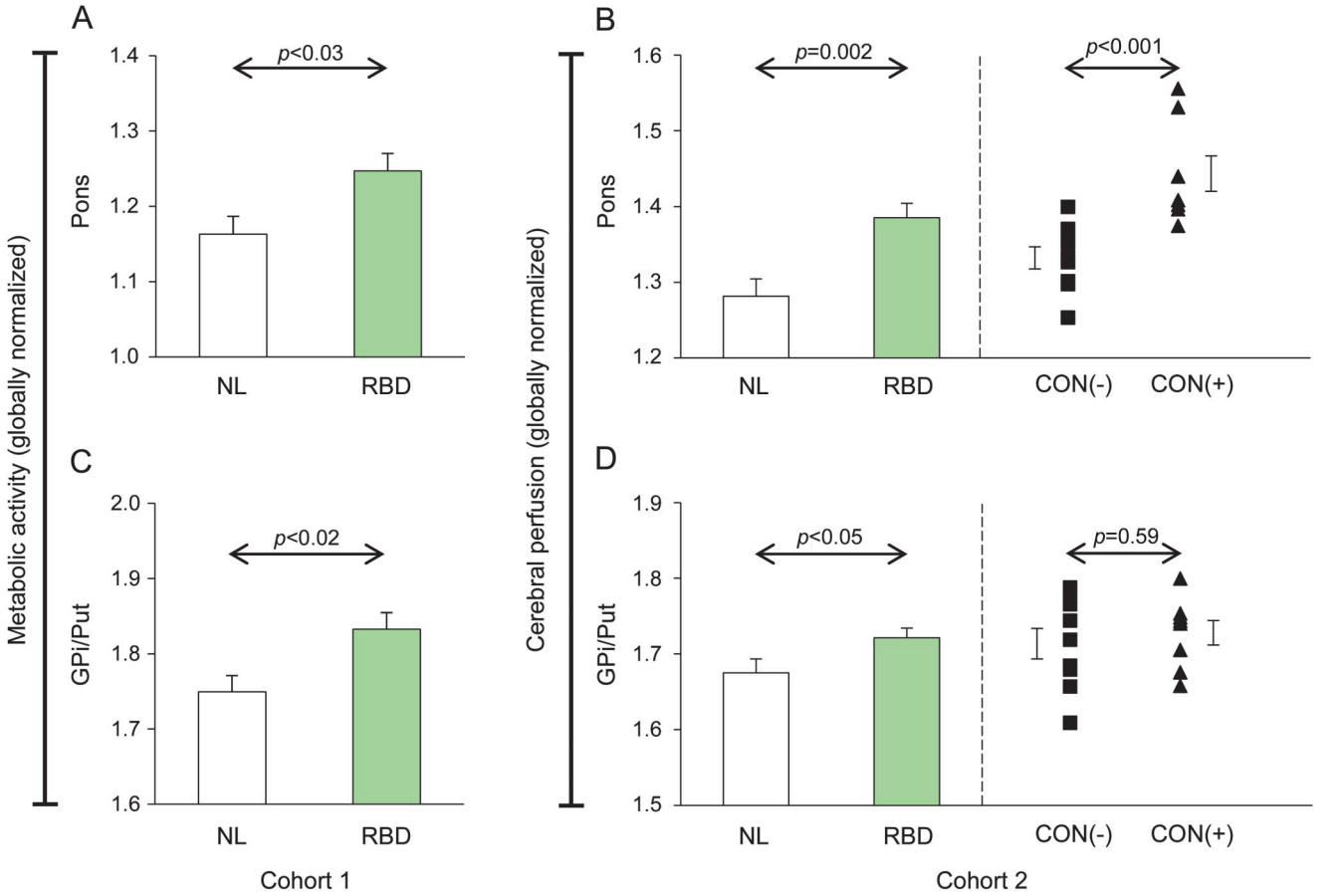

(A, B) Regional activity measured at the pontine node of the Parkinson disease–related covariance pattern network was elevated in both RBD cohorts relative to corresponding NL values (cohort 1: $p < 0.03$; cohort 2: $p = 0.002$, Student t tests). In this region (B, right panel), local activity was higher ($p < 0.001$) in the cohort 2 subjects with RBD who later phenoconverted to PD or DLB (CON[+]) than in those who did not phenoconvert (CON[−]) to a defined neurodegenerative syndrome. (C, D) Modest regional elevations ($p < 0.05$) were also noted at the putamen/GP_i node of the 2 RBD cohorts. Nonetheless, the difference between CON(+) and CON(−) subjects in cohort 2 (D, right panel) was not significant ($p = 0.59$). The error bars represent the SEM. DLB = dementia with Lewy bodies; GP_i = globus pallidus internus; NL = normal control; PD = Parkinson disease; Put = putamen; RBD = REM sleep behavior disorder.

Figure 4 Classification of subjects with RBD based on PDRP expression and age at the time of imaging

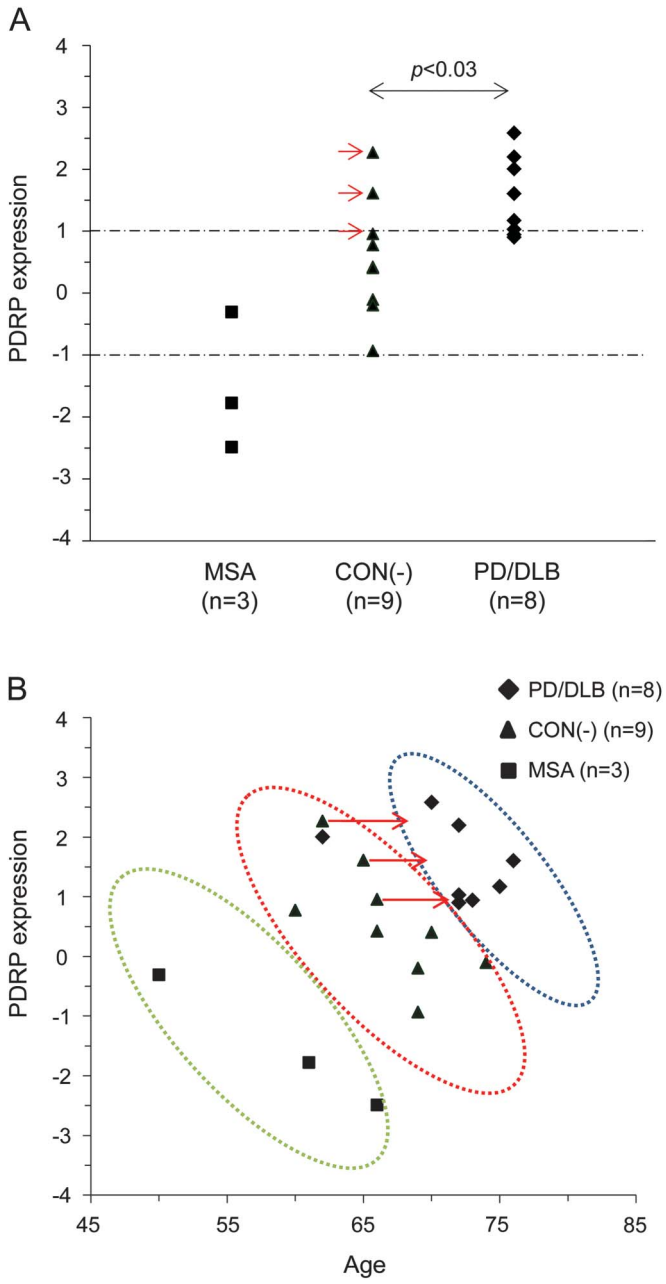

(A) PDRP expression was elevated in the cohort 2 subjects with RBD who subsequently developed clinical manifestations of PD or DLB (black diamonds) relative to those who did not phenoconvert (CON[−]) (black triangles). The 3 subjects with RBD (black squares) who subsequently developed possible or probable MSA exhibited negative network scores, indicative of expression levels that were below the normal mean. The 3 nonphenoconverters with high baseline PDRP expression are demarcated by arrows (see text). (B) Logistical regression analysis using a combination of PDRP expression values and age at the time of imaging (see methods section) accurately classified the subjects ($p < 0.0001$) as either phenoconverters to PD/DLB (blue ellipse) or MSA (green ellipse) or as nonphenoconverters (red ellipse). DLB = dementia with Lewy bodies; MSA = multiple system atrophy; PD = Parkinson disease; PDRP = Parkinson disease–related covariance pattern; RBD = REM sleep behavior disorder.

of phenoconversion in RBD. Indeed, goodness of fit improved substantially when both PDRP expression and subject age were entered together into a 2-category predictive model, accounting for 64.0% of the individual differences in phenoconversion status ($p < 0.001$). Graphical display of the data according to this model (figure 4B) revealed substantial improvement in categorization accuracy, with excellent discrimination between phenoconverters to PD/DLB (blue ellipse) and nonphenoconverters (red ellipse).

Finally, we used this approach to classify the 3 subjects with RBD who later phenoconverted to possible or probable MSA. Although the 2-category predictive model was derived from phenoconverters to PD/DLB and nonphenoconverters, the phenoconverters to MSA formed a discrete cluster (green ellipse) based on their low (subnormal) network activity and relatively young age at the time of imaging. A 3-category logistical model based on the data (figure 4B) had excellent goodness of fit, correctly classifying 19 of 20 (95%) of the subjects with RBD ($p < 0.0001$).

DISCUSSION In this study, we report elevated expression of the PDRP, an abnormal disease-related metabolic brain network, in subjects with idiopathic RBD. Indeed, significant increases in network activity were found in 2 separate RBD cohorts, at levels consistent with prodromal PD. Long-term clinical follow-up data suggested that phenoconversion was more likely in individual RBD subjects with network-level functional abnormalities at baseline.

The current study extends the prior observations of dopaminergic deficits in RBD and the relationship of these changes to incipient PD.[22,23] Of note, the PDRP network has several advantages compared with dopaminergic imaging techniques. While PDRP expression is associated with both presynaptic nigrostriatal dopaminergic dysfunction and Unified Parkinson's Disease Rating Scale motor ratings,[6,24] it is worth noting that the magnitude of these correlations is modest. Indeed, individual differences in any of these descriptors account for no more than one-third of the variation in the other 2 measures.[10] It is therefore likely that the PDRP increases seen in some subjects with RBD denote a specific functional aspect of the disease prodrome that is not captured by striatal dopamine transporter binding measurements. In this vein, the PDRP changes may also distinguish future phenoconverters to PD/DLB from MSA—conditions not readily distinguished based on dopaminergic imaging measures.[25,26] A direct comparison of dopaminergic imaging and network quantification techniques will be needed to clarify the strengths and weaknesses of the 2 scanning strategies.

It is also noteworthy that abnormal elevations in PDRP expression in subjects with RBD were observed using metabolic imaging with FDG-PET and substantiated in scans of cerebral perfusion using ECD SPECT. Indeed, we have found consistent network abnormalities in patients with PD scanned

using the latter approach.[19,20] The PDRP abnormality seen in both RBD cohorts accords well with the tight coupling that has been observed between network expression values in scans of cerebral blood flow and metabolism obtained in the same subjects.[8,27] Nonetheless, FDG-PET and ECD SPECT data are not interchangeable and thus were analyzed separately.

In aggregate, our data comport with the view of RBD as the prodromal phase of a progressive systems-based neurodegenerative process.[1–3,28] Further support is provided by the nodal measurements, which showed that regional abnormalities in the 2 RBD groups were most pronounced caudally in the pons, and that changes rostrally in the basal ganglia and thalamus were less consistent. Indeed, significant functional abnormalities were not evident in cortical PDRP network regions in either RBD cohort. This pattern is consistent with an ascending disease process.[29] Of note, we have previously reported significant metabolic abnormalities in the dorsal pons at the earliest clinical stages of PD, which increased rapidly with disease progression.[10] The underlying causes for the pontine abnormality of RBD are unknown. That this regional change was most pronounced in the phenoconverters to PD/DLB, i.e., the subjects with RBD who later developed clinical manifestations of Lewy body pathology, suggests a direct association with the neurodegenerative process itself. Nonetheless, a small nonsignificant increase in pontine activity was also present in the nonphenoconverters (figure 3B, right), compatible with the modulatory role that has been proposed for this region in the pathophysiology of RBD.[28]

While PDRP expression and subject age each provided critical information regarding the likelihood of subsequent phenoconversion, final clinical status was predicted more accurately by the 2 measures in concert. In this context, subject age proved useful as an adjunct to network activity in predicting individual case outcomes. This point is illustrated by the 3 nonphenoconverters with relatively increased PDRP expression (figure 4A, arrows). Given that these values did not differ from those of the subjects with RBD who later phenoconverted to PD/DLB, these data represent false-negative misclassifications based on the network measurements alone. We note, however, that these individuals were correctly classified once age was taken into account. Thus, despite relatively high baseline network expression levels, these subjects were likely too young for phenoconversion to have occurred during the ensuing 5 years of clinical follow-up. In fact, based on the 2-category logistical model, these individuals were unlikely to exhibit a manifest neurodegenerative phenotype for another 2 to 3 years (i.e., 4–5 years after baseline imaging; figure 4B, arrows).

Two further points are germane to network-based predictions in subjects with idiopathic RBD. First, PDRP expression was similar for RBD phenoconverters to PD and DLB (1.42 ± 0.28 [mean ± SE] and 1.79 ± 0.42, respectively). This observation is compatible with the substantial histopathologic and neurochemical overlap that has been observed between patients with PD, with or without dementia, and DLB.[30,31] Given preliminary data suggesting comparable PDRP abnormalities in patients with PD and DLB (L. Teune, personal communication), it is perhaps not surprising that the phenoconverters to PD and DLB constituted a homogeneous group regarding this particular network. Second, the 2-variable logistical model correctly classified the 3 subjects with RBD who subsequently phenoconverted to possible/probable MSA. This accords with the low PDRP expression values seen in patients with MSA.[32] Indeed, the 3 atypical phenoconverters exhibited negative subject scores, denoting subnormal network activity, which discriminated them from the other subjects with RBD. Moreover, in agreement with the earlier onset of MSA relative to PD/DLB,[33] these individuals proved to be younger than phenoconverters to PD or DLB (baseline age = 58.8 ± 8.3 years vs 71.4 ± 4.3 years). This factor, in addition to low network activity, explains the discrete clustering of the data from these subjects with RBD. Needless to say, rigorous validation studies will be needed before this or other predictive algorithms can be used reliably to predict clinical outcome in individuals with isolated RBD.

AUTHOR CONTRIBUTIONS

Dr. Holtbernd: study design, data interpretation and analysis, drafting and revision of the manuscript. Dr. Gagnon and Dr. Postuma: study design, data collection, revision of the manuscript for intellectual content. Dr. Ma and Dr. Tang: data interpretation and analysis, revision of the manuscript for intellectual content. Dr. Feigin, Dr. Dhawan, M. Vendette, and Dr. Soucy: data collection, revision of the manuscript for intellectual content. Dr. Eidelberg: study design, data interpretation and analysis, drafting and revision of the manuscript, study supervision. Dr. Montplaisir: study design, data collection, revision of the manuscript for intellectual content, study supervision.

ACKNOWLEDGMENT

The authors thank Drs. Howard Hurtig and Andrew Siderowf (Hospital of the University of Pennsylvania) for the recruitment of subjects, Dr. Thomas Chaly (The Feinstein Institute for Medical Research) for radiochemistry support, and Mr. Claude Margouleff (The Feinstein Institute for Medical Research) for technical assistance. The authors acknowledge the valuable assistance provided by Ms. Patricia J. Allen (The Feinstein Institute for Medical Research) in data analysis and by Ms. Yoon Young Choi (The Feinstein Institute for Medical Research) in copyediting.

STUDY FUNDING

Supported by the National Institute of Neurological Disorders and Stroke Morris K. Udall Center of Excellence for Parkinson's Disease Research at The Feinstein Institute for Medical Research (P50 NS071675 to D.E.), Deutsche Forschungsgemeinschaft, Fonds de Recherche du Québec—Santé, and the Canadian Institutes of Health Research. The content is

solely the responsibility of the authors and does not necessarily represent the official views of the National Institute of Neurological Disorders and Stroke or the NIH and other funding sources. The sponsor did not have a role in study design, collection, analysis and interpretation of data, writing of the report, or in the decision to submit the paper for publication.

DISCLOSURE

The authors report no disclosures relevant to the manuscript. Go to Neurology.org for full disclosures.

Received August 15, 2013. Accepted in final form November 7, 2013.

REFERENCES

1. Iranzo A, Molinuevo JL, Santamaria J, et al. Rapid-eye-movement sleep behaviour disorder as an early marker for a neurodegenerative disorder: a descriptive study. Lancet Neurol 2006;5:572–577.
2. Postuma RB, Gagnon JF, Montplaisir JY. REM sleep behavior disorder: from dreams to neurodegeneration. Neurobiol Dis 2012;46:553–558.
3. Boeve BF. REM sleep behavior disorder: updated review of the core features, the REM sleep behavior disorder-neurodegenerative disease association, evolving concepts, controversies, and future directions. Ann NY Acad Sci 2010;1184:15–54.
4. Seeley WW, Crawford RK, Zhou J, Miller BL, Greicius MD. Neurodegenerative diseases target large-scale human brain networks. Neuron 2009;62:42–52.
5. Eidelberg D. Metabolic brain networks in neurodegenerative disorders: a functional imaging approach. Trends Neurosci 2009;32:548–557.
6. Niethammer M, Eidelberg D. Metabolic brain networks in translational neurology: concepts and applications. Ann Neurol 2012;72:635–647.
7. Tang C, Poston K, Eckert T, et al. Differential diagnosis of parkinsonism: a metabolic imaging study using pattern analysis. Lancet Neurol 2010;9:149–158.
8. Ma Y, Tang C, Spetsieris P, Dhawan V, Eidelberg D. Abnormal metabolic network activity in Parkinson's disease: test-retest reproducibility. J Cereb Blood Flow Metab 2007;27:597–605.
9. Spetsieris PG, Eidelberg D. Scaled subprofile modeling of resting state imaging data in Parkinson's disease: methodological issues. Neuroimage 2011;54:2899–2914.
10. Huang C, Tang C, Feigin A, et al. Changes in network activity with the progression of Parkinson's disease. Brain 2007;130:1834–1846.
11. Tang C, Poston K, Dhawan V, Eidelberg D. Abnormalities in metabolic network activity precede the onset of motor symptoms in Parkinson's disease. J Neurosci 2010;30:1049–1056.
12. Postuma RB, Gagnon JF, Vendette M, Fantini ML, Massicotte-Marquez J, Montplaisir J. Quantifying the risk of neurodegenerative disease in idiopathic REM sleep behavior disorder. Neurology 2009;72:1296–1300.
13. Dang-Vu TT, Gagnon JF, Vendette M, Soucy JP, Postuma RB, Montplaisir J. Hippocampal perfusion predicts impending neurodegeneration in REM sleep behavior disorder. Neurology 2012;79:2302–2306.
14. Vendette M, Gagnon JF, Soucy JP, et al. Brain perfusion and markers of neurodegeneration in rapid eye movement sleep behavior disorder. Mov Disord 2011;26:1717–1724.
15. Hughes A, Daniel S, Kilford L, Lees A. Accuracy of clinical diagnosis of idiopathic Parkinson's disease: a clinico-pathological study of 100 cases. J Neurol Neurosurg Psychiatry 1992;55:181–184.
16. McKeith IG, Dickson DW, Lowe J, et al. Diagnosis and management of dementia with Lewy bodies: third report of the DLB Consortium. Neurology 2005;65:1863–1872.
17. Gilman S, Wenning G, Low P, et al. Second consensus statement on the diagnosis of multiple system atrophy. Neurology 2008;71:670–676.
18. Spetsieris P, Ma Y, Peng S, et al. Identification of disease-related spatial covariance patterns using neuroimaging data. J Vis Exp 2013;76:e50319.
19. Eckert T, Van Laere K, Tang C, et al. Quantification of Parkinson's disease-related network expression with ECD SPECT. Eur J Nucl Med Mol Imaging 2007;34:496–501.
20. Feigin A, Antonini A, Fukuda M, et al. Tc-99m ethylene cysteinate dimer SPECT in the differential diagnosis of parkinsonism. Mov Disord 2002;17:1265–1270.
21. Burnham KP, Anderson DR. Model Selection and Multimodel Inference. New York: Springer Verlag; 2002.
22. Eisensehr I, Linke R, Noachtar S, Schwarz J, Gildehaus FJ, Tatsch K. Reduced striatal dopamine transporters in idiopathic rapid eye movement sleep behaviour disorder: comparison with Parkinson's disease and controls. Brain 2000;123(pt 6):1155–1160.
23. Iranzo A, Valldeoriola F, Lomena F, et al. Serial dopamine transporter imaging of nigrostriatal function in patients with idiopathic rapid-eye-movement sleep behaviour disorder: a prospective study. Lancet Neurol 2011;10:797–805.
24. Eckert T, Tang C, Eidelberg D. Assessment of the progression of Parkinson's disease: a metabolic network approach. Lancet Neurol 2007;6:926–932.
25. Eidelberg D, Moeller JR, Ishikawa T, et al. Early differential diagnosis of Parkinson's disease with 18F-fluorodeoxyglucose and positron emission tomography. Neurology 1995;45:1995–2004.
26. Kagi G, Bhatia KP, Tolosa E. The role of DAT-SPECT in movement disorders. J Neurol Neurosurg Psychiatry 2010;81:5–12.
27. Hirano S, Asanuma K, Ma Y, et al. Dissociation of metabolic and neurovascular responses to levodopa in the treatment of Parkinson's disease. J Neurosci 2008;28:4201–4209.
28. Boeve BF, Silber MH, Saper CB, et al. Pathophysiology of REM sleep behaviour disorder and relevance to neurodegenerative disease. Brain 2007;130:2770–2788.
29. Braak H, Del Tredici K, Rub U, de Vos RA, Jansen Steur EN, Braak E. Staging of brain pathology related to sporadic Parkinson's disease. Neurobiol Aging 2003;24:197–211.
30. Klein JC, Eggers C, Kalbe E, et al. Neurotransmitter changes in dementia with Lewy bodies and Parkinson disease dementia in vivo. Neurology 2010;74:885–892.
31. Jellinger KA. A critical reappraisal of current staging of Lewy-related pathology in human brain. Acta Neuropathol 2008;116:1–16.
32. Poston K, Tang C, Eckert T, et al. Network correlates of disease severity in multiple system atrophy. Neurology 2012;78:1237–1244.
33. Ben-Shlomo Y, Wenning GK, Tison F, Quinn NP. Survival of patients with pathologically proven multiple system atrophy: a meta-analysis. Neurology 1997;48:384–393.